

Collinear Laser-rf Double-Resonance Spectroscopy: ^{235}U II Hyperfine Structure

U. Nielsen, O. Poulsen, P. Thorsen, and H. Crosswhite^(a)

Institute of Physics, University of Aarhus, DK-8000 Aarhus C, Denmark

(Received 4 August 1983)

A novel technique combining the advantages of the laser-rf double-resonance scheme and fast-beam collinear laser spectroscopy has been applied to a detailed study of the hyperfine structure of ^{235}U II. The experimental results are analyzed with use of *ab initio* Dirac-Fock calculations of the reduced radial parameters of relativistic hyperfine-structure theory. The analysis results in a new value for the nuclear dipole moment $\mu(^{235}\text{U}) = -0.38(3)\mu_N$ and a determination of the spin density $a^{10}(7s) = -2880(75)$ MHz of the $7s$ electron.

PACS numbers: 35.10.Fk, 32.30.Bv, 32.70.Jz

The application of rf spectroscopy to the investigation of ionic species has mainly developed within the last two decades. High-resolution magnetic resonance experiments have been carried out on ions in a discharge or on single ions in electrostatic traps. With the notable exception of the work of Novick and Commins¹ on ^3He II, the atomic-beam magnetic-resonance method has not been generally applied to the study of ionic species, the reason being the large inhomogeneous magnetic fields needed for state selection. This difficulty has been overcome, replacing the magnetic field state selectors with optical pumping regions,² as first demonstrated for an ion beam by Rosner *et al.*³ and later used by Kötz *et al.* to study $^6,7\text{Li}$ II.⁴

In this Letter we present a novel technique combining the advantages of laser-rf double-resonance spectroscopy⁵ and collinear fast-beam laser spectroscopy.⁶ Resolution ≈ 100 times higher than conventional collinear fast-beam laser spectroscopy is easily achieved. This is demonstrated by measurements of hyperfine structures of five odd-parity metastable levels in ^{235}U II, constituting the first high-resolution spectroscopic data of a $5f$ element. A schematic diagram of the apparatus used in this work is shown in Fig. 1. A universal ion source followed by an electrostatic accelerator and separator magnet produces a 50-keV, isotopically pure $^{235}\text{U}^+$ ion beam. A typical beam current was $0.5 \mu\text{A}$, distributed among many metastable levels belonging to the three odd configurations $5f^37s^2$, $5f^36d7s$, and $5f^36d^2$. The output from a cw ring-dye laser is superimposed on the fast-ion beam in a collinear geometry. Resonance with the fast-moving absorbers, in well-defined spatial regions, is accomplished by application of suitable voltages to floating Faraday cages surrounding the beam zones A and B, acting as postacceleration tubes.

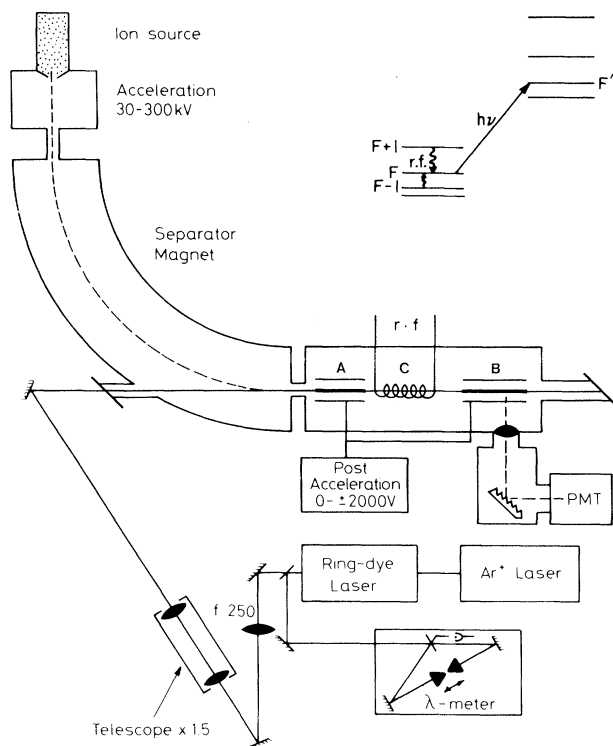


FIG. 1. The experimental apparatus consisting of an electrostatic accelerator with magnetic isotope selection and a laser spectrometer consisting of a cw ring-dye laser and λ meter. The laser field and the fast accelerated ions are superimposed in a collinear geometry with optical pumping of hyperfine level F in the initial state taking place in zone A and probing via the scattered laser photons in zone B. Zones A, B consist of Faraday cages where the ions can be Doppler tuned into resonance with the laser field. Level F can be repopulated by inducing rf transitions $F \pm 1 \rightarrow F$ in zone C and probing this rf absorption in zone B via the increase in scattered light. The optical resolution in zones A, B is ≈ 18 MHz full width at half maximum, limited by high-voltage fluctuations, and the rf resonances in zone C have a transit-time-limited full width at half maximum of ≈ 400 kHz.

Laser-induced fluorescence in zone *B* is detected by a cooled photomultiplier tube and processed through standard electronics. The velocity of the fast-moving ions is determined by means of a traveling Michelson λ meter⁶ allowing us to measure the optical Doppler shifts to within 10^{-7} . In between the pump and probe regions *A* and *B*, an rf section is inserted allowing magnetic transitions to take place in the *C* region with only an off-resonant laser field present. The rf field is produced in a 50- Ω impedance-matched coaxial transmission line. This design has been chosen in order to insure a uniform field distribution over an appreciable length (length of interaction 47.5 cm) and a simple field configuration, consisting of one traveling TEM mode along the beam axis. The entire rf section is surrounded by a Mumetal shield, reducing the ambient static magnetic field to ≈ 5 mG. For a 50-keV $^{235}\text{U}^+$ beam, the transit-time broadening thus becomes the sole observable contributor to the linewidth.

The laser-rf double-resonance scheme is well discussed in the literature³⁻⁵ and only a brief outline, with emphasis on specific features of this experiment, will be given here. The Faraday cages *A* and *B* act as pumping and probing zones, respectively. With appropriate voltages applied to them, the laser field will be resonant on *one* particular $F-F'$ hfs transition in both zones. The effect of the resonant light in zone *A* is a depletion of the population of level F due to optical pumping. This is observed in zone *B* as a reduction of the laser-induced fluorescence monitored by the photomultiplier tube. Application of an rf field resonant on the transitions $F \pm 1 \rightarrow F$ to the rf section *C* will repopulate the level F , depleted in zone *A*, with an increase of the number of scattered photons in probe zone *B* as a consequence. This allows a direct determination of the hfs splittings $(F \pm 1)-F$. In this setup a collinear geometry was chosen for the following reasons: As a result of the low beam current available and the distribution of the ions on many different metastable states, an appreciable depopulation in zone *A* is necessary in order to obtain a good signal-to-noise ratio. For a 50-keV $^{235}\text{U}^+$ beam this demands an interaction length of several centimeters, difficult to obtain in a crossed-beam geometry. Moreover, because of the longitudinal velocity compression, yielding optical resolution below 20 MHz in our experiment, a major part of the ion beam will participate in the laser-rf double-resonance process thus further enhancing the obtainable signal-to-noise ratio. This

feature also has the important consequence that spurious signals due to interaction with different velocity groups in zones *A* and *B* are readily avoided.

With an interaction length of 30 cm between laser field and ions in zone *A* (this corresponds to ~ 1.5 μsec) and laser power 0.3 W/cm^2 , a 40%–50% reduction of scattered photons in zone *B* was typically achieved. Half of this depletion could be pumped back by a few watts of rf power, thus allowing data collection times on the order of a few minutes for each rf spectrum of the type shown in Fig. 2. The measured transition frequencies have been corrected for Doppler shifts on the order of 50–500 kHz. The fitted line shape is the Rabi solution for the inversion in a two-level system with the experimental full width at half maximum found in this way being in good agreement with the transit-time limit dictated by an interaction length of 47.5 cm and a 50-keV $^{235}\text{U}^+$ beam.

The single most important systematic effect is the dependence of the measured rf-transition frequencies on the applied post acceleration, this being a direct measure of the detuning of the laser field in the rf region *C*. No ac Stark shifts of the resonances were observed within our limit of uncertainty. This is consistent with a calculation

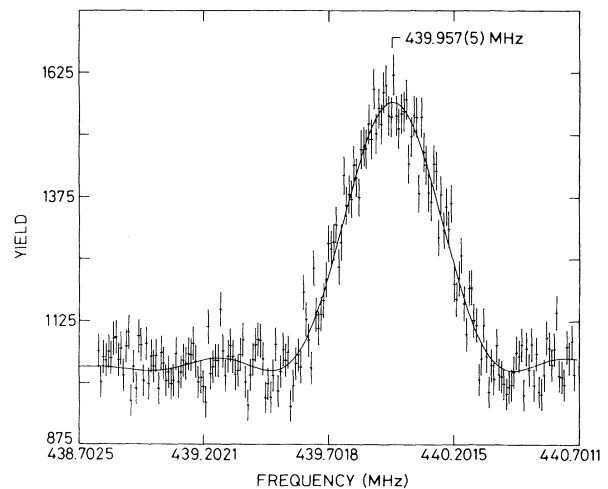


FIG. 2. A typical rf resonance, observed in the $F = 6-7$ transition in the 5790 cm^{-1} , $J = \frac{11}{2}$ level. The rf power used was 6 W, corresponding to an oscillating magnetic field of 25 mG. The associated Rabi-flopping frequency (cyclic) of $\Omega \approx 600$ kHz corresponds to a transition probability of 30% in zone *C*. The solid line represents a fit to the data using the transit-time-limited line shape $\sin^2[(\Omega^2 + \Delta^2)^{1/2}t]/(\Omega^2 + \Delta^2)$, where Δ is the detuning and $2t$ the interaction time.

of the optical Rabi frequencies inferred from lifetime measurements performed earlier.⁶ With a post acceleration voltage of 300 V, corresponding to a frequency detuning of ≈ 1 GHz, an ac Stark shift of the rf resonance of the order of 100 Hz is calculated.

The results of our measurements are summarized in Table I. The quoted hfs coupling constants represent least-squares adjustments to the observed hyperfine intervals and are not corrected for second-order hfs. Together with optical data, obtained for seven other levels, by use of fast-beam collinear laser spectroscopy, these results have been analyzed within the Sandars-Beck formalism⁷ of relativistic hyperfine-structure theory. To obtain the needed intermediate-coupling wave functions, fine-structure levels^{8,9} of U II have been fitted to a model¹⁰ which contains electrostatic and spin-orbit interactions for the complete manifold of the lowest three odd configurations, f^3s^2 , f^3ds , and f^3d^2 . Twenty-one parameters were allowed to vary in order to fit sixty known odd levels, with other parameters fixed at values consistent with Hartree-Fock calculations or extrapolated from other spectroscopic information. Eigenvectors from the diagonaliza-

TABLE I. hfs intervals measured with collinear fast-beam rf-laser double-resonance spectroscopy. The listed magnetic dipole (electric quadrupole) interaction constants A (B) represent least-squares fits to these hfs intervals, using the zeroth-order spin Hamiltonian (Ref. 7). No second-order hfs corrections have been applied. The uncertainty on ν_0 is 10 kHz.

Level _{<i>J</i>} (cm ⁻¹)	<i>F-F</i>	ν_0 (MHz)	<i>A</i> (MHz)	<i>B</i> (MHz)
4585 _{13/2}	6-7	231.720	9.546(3)	3105.1(10)
	7-8	76.334		
	8-9	520.990		
5401 _{7/2}	3-4	322.726	-60.301(6)	400.1(2)
	4-5	342.494		
	5-6	321.252		
	6-7	250.274		
5790 _{11/2}	5-6	380.885	62.753(3)	-37.4(1)
	6-7	439.959		
	7-8	496.967		
	8-9	551.642		
6445 _{9/2}	2-3	469.419	-235.010(3)	-1276.9(10)
	3-4	696.822		
	4-5	985.044		
7166 _{9/2}	4-5	338.360	-107.843(6)	-1349.6(10)
	5-6	582.834		
	6-7	923.580		

tion were then used to transform the hfs matrix elements for these three configurations to intermediate coupling. The second ingredient in the hfs analysis is the relativistic one-electron integrals⁷ $F_{jj'}$, which have been calculated by use of a multiconfigurational Dirac-Fock procedure^{11,12} with the finite size of the 235-uranium nucleus represented by a Fermi surface.¹³ For the non-*s* electrons the relativistic effects on these integrals amount to 10%-20%,¹² whereas the $F_{jj'}$ integral $\int (P_j Q_{j'} + Q_j P_{j'}) r^{-2} d\mathbf{r}$ for the 7*s* electron is highly relativistic as well as strongly dependent on the nuclear potential. P (Q) is the large (small) component of the Dirac wave function. Thus the experimental data for the magnetic dipole interaction have been least-squares adjusted to a model with $F_{jj'}(7s)$ and the nuclear magnetic dipole moment μ of 235 uranium as variable parameters. The calculated values for $F_{jj'}(5f)$ and $F_{jj'}(6d)$ were used in this analysis, the reason being their small contributions to the dipole coupling constants A as compared to the dominant $F_{jj'}(7s)$ contribution. For the metastable levels below 6000 cm⁻¹ of excitation energy the experimental measured A values are fitted to within 2% with $\mu(^{235}\text{U}) = -0.38(3)\mu_N$ and the Fermi-coupling constant $a^{10}(7s) = -2880(75)$ MHz.

The value $\mu = -0.38(3)\mu_N$ is slightly larger than previous determinations¹⁴ with electron-nuclear double resonance ($\mu = -0.36$) and electron paramagnetic resonance ($\mu = -0.35$). In our analysis, the extended nuclear magnetization,¹⁵ estimated to be +3%, has not been included due to the 10% uncertainty in the eigenvectors. Its inclusion increases the discrepancy with the previous μ determinations. However, the high internal consistency in our analysis shows that nuclear moments indeed can be evaluated from optical data for these complicated actinide elements.

The Fermi-coupling constant $a^{10}(7s)$, given by $a^{10}(7s) = 4980\mu F_{1/2\ 1/2}(7s)$, allows an experimental determination of $F_{1/2\ 1/2}(7s) = 1.52(8)$ a.u. The Dirac-Fock value $F_{1/2\ 1/2}(7s) = 1.43$ a.u. has been calculated with the coupling scheme¹⁰ $\{(5f^3\ ^4I)J_1, (6d^2\ ^2D)J_2, (7s^2\ ^1S)\frac{1}{2}\}J$ and with the total wave function a linear combination of configuration state functions that are eigenstates of parity, J^2 , and J_z . The effect of introducing the Fermi surface of the uranium-235 nucleus decreases the Dirac-Fock value of $F_{1/2\ 1/2}(7s)$ by $\sim 30\%$ as compared to a point nucleus, whereas the variation of $F_{1/2\ 1/2}(7s)$ over the various J values only amounts to $\sim 2\%$.

This study thus clearly demonstrates that the

introduction of new high-resolution methods allows us an insight into the complex actinide elements, complementary to classical Doppler-limited spectroscopy.^{8,9} Eigenvectors based on such classical spectroscopy, Dirac-Fock calculations,¹¹ and high-resolution collinear fast-beam rf-laser double-resonance spectroscopy have permitted a detailed analysis of the magnetic hyperfine structure in the three odd configurations of ²³⁵U II. This analysis takes advantage of the pure intermediate-coupling wave functions characteristic of the *ion* as compared to the atom, although they do not allow the analogous analysis of the electric quadrupole interaction at present. This work was supported by the Danish Natural Science Research Council.

(a)Permanent address: Argonne National Laboratory, Argonne, Ill. 60439.

¹R. Novick and E. D. Commins, Phys. Rev. 111, 822 (1958).

²S. D. Rosner, R. A. Holt, and T. D. Gaily, Phys. Rev. Lett. 35, 785 (1975).

³S. D. Rosner, T. D. Gaily, and R. A. Holt, Phys.

Rev. Lett. 40, 851 (1978).

⁴U. Kötzt, J. Kowalski, R. Neumann, S. Noehte, H. Suhr, K. Winkler, and G. zu Putlitz, Z. Phys. A 300, 25 (1981).

⁵W. J. Childs, O. Poulsen, L. S. Goodman, and H. Crosswhite, Phys. Rev. A 19, 168 (1979).

⁶O. Poulsen, T. Andersen, S. M. Bentzen, and U. Nielsen, Phys. Rev. A 24, 2523 (1981).

⁷I. Lindgren and A. Rosén, Case Stud. At. Phys. 4, 93 (1974).

⁸D. W. Steinhaus, L. R. Radziemski, Jr., R. D. Cowan, J. Blaise, G. Guelachvili, Z. Ben Osman, and J. Vergés, Los Alamos Scientific Laboratory Report No. LA-4501, 1971 (unpublished).

⁹B. A. Palmer, R. A. Keller, and R. Engleman, Jr., Los Alamos Scientific Laboratory Report No. LA-8251-MS, 1981 (unpublished).

¹⁰R. D. Cowan, *The Theory of Atomic Structure and Spectra* (Univ. California Press, Berkeley, 1981).

¹¹J. P. Desclaux, Comput. Phys. Commun. 9, 31 (1975).

¹²J. P. Desclaux, At. Data Nucl. Data Tables 12, 311 (1973).

¹³M. A. Preston and R. K. Bhaduri, *Structure of the Nucleus* (Addison-Wesley, Reading, Mass., 1975).

¹⁴C. M. Lederer and V. S. Shirley, *Tables of Isotopes* (Wiley, New York, 1978).

¹⁵T. Fujita and A. Arima, Nucl. Phys. A254, 513 (1975).